

Aircraft Vibration Detection and Diagnosis for Predictive Maintenance using a GLR Test

S. Urbano*, E. Chaumette**, P. Goupil*, J-Y. Tourneret***

* Airbus, 316 route de Bayonne, 31060, Toulouse, France

** ISAE/TéSA, 10 Avenue Edouard-Belin, 31055, Toulouse, France

*** ENSEEIHT/TéSA, 2 rue Charles Camichel, 31071, Toulouse, France

Abstract: This paper studies a statistical approach to detect and diagnose a particular type of vibration impacting the control surfaces of civil aircraft. The considered phenomenon is called Limit Cycle Oscillation (LCO). It consists of an unwanted sustained oscillation of a control surface due to the combined effect of aeroelastic phenomena and an increased level of mechanical free play in the elements that connect the control surface to the aerodynamic surface. The state-of-the-art for LCO prevention is mainly based on regular free play checks performed on ground during maintenance operations. The detection is mainly achieved by the crew, and especially the pilot who can fill in a so-called “vibration reporting sheet” to describe the phenomena felt during the flight. Thus, the pilot sensitivity to vibration is still the only reference for LCO detection. In the Flight Control System (FCS) of modern aircraft there exist already several certified algorithms for the detection of vibrations of different nature, which use dedicated local sensors to monitor the control surface behaviour. The same kind of sensors have been chosen in a local approach, which eases the isolation of the vibration sources. This paper studies a new statistical approach based on the Generalized Likelihood Ratio Test (GLRT) in order to improve the state-of-the-art for LCO detection and diagnosis. The test and its theoretical performance are derived and validated. A straightforward method compliant with real-time implementation constraint for LCO prediction is proposed. A Monte Carlo test campaign is performed in order to assess the robustness and the detection/diagnosis performance of the proposed algorithm under different operating conditions.

Keywords: Flight Control, Fault Detection and Isolation, Predictive Maintenance, Limit Cycle Oscillation, Generalized Likelihood Ratio Test.

1. INTRODUCTION

Spurious oscillations of the control surfaces (C/S) of a civil aircraft impact both the structural airframe design and the flight control system design. Indeed, undetected oscillations may lead to local structural load augmentation, flight handling qualities deterioration, actuator operational life reduction, cockpit and cabin comfort deterioration, maintenance cost augmentation. For this reason, the ability to detect and isolate unwanted oscillations beyond a given amplitude (in a given time depending on the fault type) is an important feature for a fault-tolerant, economically efficient and comfortable aircraft architecture. The causes of C/S oscillation can be internal to the Flight Control system (faulty behaviour of an electronic component or a mechanical failure) and they are generally referred as Oscillatory Failure Case (OFC) (Goupil, 2010). However, they can also be external (aerodynamic non-linearities as shock waves) or partially internal and external. It is the case of aeroservoelastic oscillations (Dowell, 2014) known as Limit Cycle Oscillations (LCO). The state-of-the-art concerning OFC detection is mainly based on analytically redundancy approaches (Goupil, 2010)(Zolghadri et al., 2013) while LCO detection to the best of author’s knowledge still depends almost entirely on crew sensitivity to

vibrations. The idea to use statistical and data-driven technique for C/S oscillation detection has also been investigated in the literature. For example, in (Zolghadri et al., 2013) and (Simon, 2011), a few data-driven approaches are discussed for OFC detection. These approaches include a fault modelling strategy based on Kalman filtering or using a specific observer, selective filtering, correlation methods, synchronous detection. In (Goupil et al., 2016) and (Urbano et al., 2017a) an OFC detection algorithm is also proposed based on distance and correlation measures. In the present paper a different approach based on a likelihood ratio test (LRT) is investigated for the problem of LCO detection and diagnosis.

Generalized Likelihood Ratio Tests (GLRT) are standard tools for the detection of deterministic signals with unknown parameters due to their simple structure, wide applicability and optimal asymptotic performance (Kay, 1998). For this reason, the authors of the present paper have decided to propose a simple detection algorithm based on the GLRT and a simple modelling of the control surface servo loop. A simple method compliant with real-time implementation constraints for LCO diagnostic results from this algorithm.

The paper is organized as follows: Section 2 presents the

state-of-the-art concerning LCO prevention and detection. Section 3 introduces the GLRT method and its derivation with the proposed hypotheses. Section 4 proposes a simple approach for LCO diagnostic resulting from the GLRT. Section 5 presents some results of a Monte Carlo test campaign realized using an Airbus simulator. These results show the robustness and detection performance under different operating conditions. Section 6 summarizes conclusions and describes some perspectives of this study.

2. STATE-OF-THE-ART

The first events of control surface flutter and LCO occurred during the 1st World War and the most widely adopted solution was to consider control surface mass balancing (Von Baumhauer and Koning, 1923). In 80-90s, the hydraulic actuators became reliable enough to ensure the aeroelastic stability by their own stiffness or damping. For this reason, the C/S mass balancing was given up because of its drag and weight penalty (Dowell, 2014). Unfortunately, this solution presents a weak point: with the cumulative wear (aircraft ageing), some supporting elements of control surface develop mechanical free play and so the C/S can vibrate inside its free play. For this reason, the actuator stiffness solution has often to be coupled with other countermeasures such as

- i) low free play articulation technologies (roller bearings for example)
- ii) free play monitoring via periodic maintenance check
- iii) control surface artificial static loading (achieved by specific devices or by the actuators linked to the C/S)
- iv) in-flight LCO monitoring
- v) in-flight LCO adaptive control (Livne, 2017)

It is important to note that i), ii), iii) concern LCO prevention, while iv) and v) consider directly the problem of LCO detection and control. The current study is intended to propose a new method in the context of iv) where the state-of-the-art is often based only on the pilot sensitivity to vibrations. Indeed, after each flight, the crew can fill in a so-called ‘‘Vibration Reporting Sheet’’ (Airbus) or a ‘‘Flight Deck Vibration Event Log’’ (Boeing) to describe the phenomena felt during the flight, clearly leading only to qualitative information about the phenomenon.

In the Airbus architecture, the servo loop that moves the control surface (see Fig. 1) is already monitored by several fault detection algorithms (Goupil, 2010). Thus, it is interesting to investigate the possibility of using a statistical approach for LCO detection and diagnosis (based on existing measurement and compliant with real-time implementation constraints).

3. GENERALIZED LIKELIHOOD RATIO TEST

The control surface servo loop in Fig. 1 can be modeled as in Fig. 2, where \mathbf{x} is the command sent to the actuator from the flight control system, P represents the actuator dynamic, \mathbf{s} is the oscillation to be detected (it is present only under the hypothesis \mathcal{H}_1), \mathbf{y} is the measured control surface position and \mathbf{w} is the measurement noise. In this study we will consider that the noise power is known and that \mathbf{x} and \mathbf{y} are known. For a very simple model of the actuator dynamic of the type $\mathbf{y}^0 = \lambda \mathbf{x}(n-p)$, where λ is an attenuation/amplification factor and p is a delay, the LCO detection problem can be expressed by the following binary hypothesis testing problem

$$\begin{cases} \mathcal{H}_0 : y(n) &= \lambda x(n-p) + w(n) \\ \mathcal{H}_1 : y(n) &= \lambda x(n-p) + A \cos(2\pi f n + \phi) + w(n) \end{cases} \quad (1)$$

where $n = 0, \dots, N-1$ and $w(n) \sim \mathcal{N}(0, \sigma^2)$. The signal to detect $\mathbf{s}(n) = A \cos(2\pi f n + \phi)$ can be rewritten as

$$s(n) = l_1 \cos(2\pi f n) + l_2 \sin(2\pi f n) \quad (2)$$

allowing the non linear dependency with respect to ϕ to be removed. In this case $A = \sqrt{l_1^2 + l_2^2}$ and $\phi = \arctan(\frac{-l_2}{l_1})$. The problem in (1) is a problem of deterministic signal detection in interference (Kay, 1998), where $\mathbf{s}(n)$ is the signal to detect and $\lambda \mathbf{x}(n-p)$ is the interference.

The following conditional model (CM) (Stoica and Nehorai, 1990) can be considered to derive the detector

$$\begin{cases} \mathcal{H}_0 : \mathbf{y} = \mathbf{H}_0(\boldsymbol{\alpha}_0) \boldsymbol{\beta}_0 + \mathbf{w} \\ \mathcal{H}_1 : \mathbf{y} = \underbrace{[\mathbf{H}_0(\boldsymbol{\alpha}_0) \quad \mathbf{H}_s(\boldsymbol{\alpha}_s)]}_{\mathbf{H}_1(\boldsymbol{\alpha}_1)} \underbrace{\begin{bmatrix} \boldsymbol{\beta}_0 \\ \boldsymbol{\beta}_s \end{bmatrix}}_{\boldsymbol{\beta}_1} + \mathbf{w} \end{cases} \quad (3)$$

where $\boldsymbol{\alpha}_0 = [p]$, $\boldsymbol{\beta}_0 = [\lambda]$, $\boldsymbol{\alpha}_1 = [p, f]^T$, $\boldsymbol{\beta}_1 = [\lambda, l_1, l_2]^T$ and the observation matrices are

$$\mathbf{H}_0(\boldsymbol{\alpha}_0) = \mathbf{x}(p) = \begin{pmatrix} x(-p) \\ x(1-p) \\ \vdots \\ x(N-1-p) \end{pmatrix}$$

$$\mathbf{H}_1(\boldsymbol{\alpha}_1) = [\mathbf{x}(p) \quad \mathbf{c}(f) \quad \mathbf{s}(f)] =$$

$$\begin{bmatrix} x(-p) & 1 & 0 \\ x(1-p) & \cos(2\pi f) & \sin(2\pi f) \\ \vdots & \vdots & \vdots \\ x(N-1-p) & \cos(2\pi f(N-1)) & \sin(2\pi f(N-1)) \end{bmatrix}$$

In a two hypothesis testing problem, the optimal decision rule is based on the exact statistics of the observations. Its expression requires knowledge of the Probability Density Function (PDF) of observations under each hypothesis and the a priori probability of each hypothesis, if known (Bayes criterion). If no a priori probability of hypotheses is available, then most often used criterion is the likelihood ratio test (LRT) derived by Neyman-Pearson (Kay, 1998). Unfortunately, optimal statistical tests such as the LRT cannot always be implemented since there are often some unknown parameters in the observation model, leading to the so-called composite hypothesis testing problem (Van Trees, 2004) (also referred to as joint detection estimation problem (Galy et al., 2010)). A very common approach in this situation is to replace the unknown parameters in the LRT by their maximum likelihood estimators (MLE), following the ideas of the generalized likelihood ratio test (GLRT) (Van Trees, 2004). It is known that the GLRT does not generally keep the optimal properties of the LRT. However, the GLRT approach has several advantages: the test is often easy to derive and sometimes its expression and distribution can be determined analytically (Kay, 1998), it is known to be the uniformly most powerful (UMP) test for some classes of problems in the asymptotic region (Scharf and Friedlander, 1994).

The GLRT requires to estimate the unknown parameter vectors $\boldsymbol{\alpha}_i$ and $\boldsymbol{\beta}_i$ under both hypotheses (i.e., for $i = 0, 1$) using the maximum likelihood principle. Considering the hypothesis of additive white Gaussian noise of known

variance σ^2 ($w(n) \sim \mathcal{N}(0, \sigma^2)$), the likelihood of the observed vector \mathbf{y} is

$$p(\mathbf{y}; \boldsymbol{\alpha}, \boldsymbol{\beta}) = \frac{1}{(2\pi\sigma^2)^{\frac{N}{2}}} \exp\left(-\frac{1}{2\sigma^2} \|\mathbf{y} - \mathbf{H}(\boldsymbol{\alpha})\boldsymbol{\beta}\|^2\right).$$

As a consequence, the GLRT can be written as

$$\frac{p(\mathbf{y}; \boldsymbol{\alpha}_1, \boldsymbol{\beta}_1 | \mathcal{H}_1)}{p(\mathbf{y}; \boldsymbol{\alpha}_0, \boldsymbol{\beta}_0 | \mathcal{H}_0)} = \frac{\exp\left(-\frac{1}{2\sigma^2} \|\mathbf{y} - \mathbf{H}_1(\hat{\boldsymbol{\alpha}}_1)\hat{\boldsymbol{\beta}}_1\|^2\right)}{\exp\left(-\frac{1}{2\sigma^2} \|\mathbf{y} - \mathbf{H}_0(\hat{\boldsymbol{\alpha}}_0)\hat{\boldsymbol{\beta}}_0\|^2\right)} \underset{\mathcal{H}_1}{\underset{\mathcal{H}_0}{\lesseqgtr}} \gamma.$$

The estimation problem, considering a general notation that is true for both the hypotheses \mathcal{H}_0 and \mathcal{H}_1 , reduces to the minimization of following least squares (LS) criterion (Kay, 1993)

$$\mathbf{J}(\boldsymbol{\alpha}, \boldsymbol{\beta}) = \|\mathbf{y} - \mathbf{H}(\boldsymbol{\alpha})\boldsymbol{\beta}\|^2 = (\mathbf{y} - \mathbf{H}(\boldsymbol{\alpha})\boldsymbol{\beta})^T (\mathbf{y} - \mathbf{H}(\boldsymbol{\alpha})\boldsymbol{\beta}).$$

The value of $\boldsymbol{\beta}$ that minimizes $\mathbf{J}(\boldsymbol{\alpha}, \boldsymbol{\beta})$ for a given value of $\boldsymbol{\alpha}$ is

$$\boldsymbol{\beta} = (\mathbf{H}^T(\boldsymbol{\alpha})\mathbf{H}(\boldsymbol{\alpha}))^{-1}\mathbf{H}^T(\boldsymbol{\alpha})\mathbf{y} \quad (4)$$

and replacing this value of $\boldsymbol{\beta}$ in $\mathbf{J}(\boldsymbol{\alpha}, \boldsymbol{\beta})$, we obtain the following MLE of $\boldsymbol{\alpha}$

$$\hat{\boldsymbol{\alpha}} = \underset{\boldsymbol{\alpha}}{\operatorname{argmin}} \|\Pi_{\mathbf{H}}^\perp \mathbf{y}\|^2. \quad (5)$$

where $\Pi_{\mathbf{H}} = \mathbf{H}(\mathbf{H}^T\mathbf{H})^{-1}\mathbf{H}^T$ is the orthogonal projection matrix that projects a vector onto the columns of \mathbf{H} , and $\Pi_{\mathbf{H}}^\perp = \mathbf{I} - \Pi_{\mathbf{H}}$ is the projection matrix that projects a vector onto the space orthogonal to the columns of \mathbf{H} . The sufficient statistic T for the GLRT is therefore

$$T = \frac{1}{2\sigma^2} \left(\|\mathbf{y} - \mathbf{H}_0(\hat{\boldsymbol{\alpha}}_0)\hat{\boldsymbol{\beta}}_0\|^2 - \|\mathbf{y} - \mathbf{H}_1(\hat{\boldsymbol{\alpha}}_1)\hat{\boldsymbol{\beta}}_1\|^2 \right) \quad (6)$$

$$= \frac{1}{2\sigma^2} \left(\|\Pi_{\mathbf{H}_0(\hat{\boldsymbol{\alpha}}_0)}^\perp \mathbf{y}\|^2 - \|\Pi_{\mathbf{H}_1(\hat{\boldsymbol{\alpha}}_1)}^\perp \mathbf{y}\|^2 \right) \underset{\mathcal{H}_1}{\underset{\mathcal{H}_0}{\lesseqgtr}} \gamma \quad (7)$$

Observing that $\Pi_{\mathbf{H}}^\perp = \mathbf{I} - \Pi_{\mathbf{H}}$, we can also obtain the following equivalent detector

$$T'' = \|\Pi_{\mathbf{H}_1(\hat{\boldsymbol{\alpha}}_1)} \mathbf{y}\|^2 - \|\Pi_{\mathbf{H}_0(\hat{\boldsymbol{\alpha}}_0)} \mathbf{y}\|^2 \underset{\mathcal{H}_1}{\underset{\mathcal{H}_0}{\lesseqgtr}} 2\sigma^2\gamma. \quad (8)$$

Concerning the detector performance, it can be proved (Urbano et al., 2017b), that for the problem in (1) we obtain the following expressions of the false alarm probability P_{FA} and detection probability P_D for one observation window

$$P_{\text{FA}} = P(2T > \gamma | H_0) = P(\chi_r^2 > \gamma) = Q_{\chi_r^2}(\gamma)$$

$$P_D = P(2T > \gamma | H_1) = P(\chi_r^2(k) > \gamma) = Q_{\chi_r^2(k)}(\gamma) \quad (9)$$

where the functions $Q_{\chi_r^2}$ and $Q_{\chi_r^2(k)}$ are the complementary cumulative distribution functions of central and non central chi square distributions¹ whose parameters r and k are detailed in Appendix A. It is important to observe that starting from the theoretical expression of the detection performance (9), one can tune the threshold γ directly for a given constant false alarm rate. Indeed, one can choose

$$\gamma = Q_{\chi_r^2}^{-1}(P_{\text{FA}}) \quad (10)$$

where for M non-overlapping windows (white noise) one can simply consider $P_{\text{FA}} = \prod_{i=1}^M P_{\text{FA}}^i$ (for $P_{\text{FA}} \ll 1$). Furthermore, being the expression of P_D a function of

¹ whose closed form expressions can be found for example in (Kay, 1998, Chap. 2)

the observation window dimension N (through the chi-square non centrality parameter k , see Appendix A), one can choose N in order to maximize the P_D (respecting the constraints, if any, in terms of hardware limits or detection time).

Remark 1: simple expressions for the MLEs and the test statistic can be obtained for the case in (1). These expressions (detailed in Appendix B) can be implemented in an auto-recursive scheme, reducing considerably the overall computational cost of the method. Moreover, the optimization process required in (5) can be simplified considering the so-called Alternating Projection approach as in (Ziskind and Wax, 1988).

Remark 2: if we are looking to reduce further the computational burden of the method, one can consider some specific cases. For example, if we already know some (or all) the parameters $\boldsymbol{\alpha}$ in (3), we can simplify the test structure and avoid the optimization process in (5). Moreover, it is clear that if the signal \mathbf{x} does not contain any signal component at the frequency f , the test statistic reduces to the simple periodogram of \mathbf{y} (the signal \mathbf{x} does not bring any useful information for the detection and the power spectrum of \mathbf{y} is all we need to detect \mathbf{s}). This can be also verified looking at the equations in Appendix B.

4. VIBRATION DIAGNOSTIC

The GLRT defined in the previous section implicitly involves the estimation of the LCO amplitude $\hat{A} = \sqrt{\hat{l}_1^2 + \hat{l}_2^2}$ and duration² $\widehat{\Delta T}$. This means that we can estimate the energy produced by the vibration as

$$\hat{E}_{\text{LCO}} = \int_{\widehat{\Delta T}} \hat{A}^2 dt.$$

Based on this observation, a very simple method for vibration diagnostic can be proposed. Indeed, if we consider that only a fraction of E_{LCO} is dissipated through wear process that increase the free play level, we can define a simple diagnostic index I (for a given flight F) as

$$I(F) = k_w \int_{\widehat{\Delta T}_F} \hat{A}_F^2 dt$$

where k_w is a wear severity coefficient. At this point, this definition of I can be easily extended to n flights by considering a recursive expression of the type

$$I(F_n) = \lambda_f I(F_{n-1}) + k_w \int_{\widehat{\Delta T}_{F_n}} \hat{A}_{F_n}^2 dt \quad (11)$$

where λ_f is a forgetting factor adjusted to reduce the undesired effects of estimation errors. The vibration diagnostic index (11) provides a rough estimate of the system deterioration due to vibrations (free play increase) and thus it can be used for diagnostic purpose on a control surface. However, it is important to observe that the simple expression (11) has to be coupled with a relevant threshold to be meaningful, which may be a tricky task. Indeed, one can choose to link empirically the index I with an acceptable level of cabin and cockpit comfort. However, this concept may vary between pilots and airlines. For this reason, in the next section we will focus only on the estimation accuracy in terms of LCO amplitude and

² The signal is detected in M observation windows of dimension N . If T_s denotes the sampling period, we can approximate the duration as $\widehat{\Delta T} = MNT_s$.

duration, leaving the computation of I and the associated threshold tuning to further studies. Note also that the parameters k_w and λ_f may be considered as time-varying for a more accurate prediction of the vibration evolution. Concerning the interaction between wear process and limit cycle oscillations, the reader can find an interesting description in (Safi et al., 2002), where wear models and predictive equations are presented and where it is shown that the sliding wear damage has a predominant effect compared to the impact wear damage. Moreover, it is observed that, if a vibration occurs, the rate of development of the free play can increase exponentially.

5. RESULTS

A Monte Carlo test campaign has been conducted using an industrial Airbus desktop simulator to evaluate the detection performance of the proposed approach. A test set, composed of the signals x and y , has been generated for the elevator of a specific Airbus aircraft that flies on the typical mission profile for that aircraft (see Fig. 7) under different operating conditions in terms of Mass, balance, Mach number and turbulence level³ (see Table 1). Various possible operating conditions (around 2500) have been simulated based on the typical profile mission in Fig. 7 and a particular combination of the parameters in Table 1. A simplified version of the algorithm described in Section 3 has been considered for hardware capacity reasons (see Appendix B for more details). In fact, we cannot guarantee the absence of signal power at the frequency f in \mathbf{x} . However, we can consider that the power of the sinusoid is small compared to the energy and covariance terms $\mathbf{x}^T(\hat{p})\mathbf{x}(\hat{p})$ and $\mathbf{x}^T(\hat{p})\mathbf{y}$, leading to $\hat{p}_0 \approx \hat{p}_1 \approx \hat{p}$. In this case, the estimation of the system dynamic P and the detection of the oscillation \mathbf{s} can be decoupled reducing the computational cost of the algorithm. In other terms, we have reduced the algorithm to a simple two step approach of the type estimation plus detection (recursive estimation of the system dynamic for residual generation plus sinusoidal detection on the residuals). The system dynamic can be estimated based on the MLEs under \mathcal{H}_0 , while the detection problem reduces to the surveillance of the power spectral density of the residuals. Note that the LCO frequency f is generally known a priori based on the aeroelastic properties of the system, so the frequency band to be monitored is narrow.

The threshold can be tuned based on (10) for a $P_{\text{FA}} = 10^{-t}$ for flight hour, where $t \in [3, 6]$ and $r = 2$ under the considered hypotheses. Based on (9), the observation window has been chosen as the smallest one able to detect a given vibration amplitude A_1 (lower than pilot sensitivity) with P_D close to one (for the given P_{FA}). A value of 10 seconds has been chosen for the observation window, based on a sampling rate of $F_s = 100\text{Hz}$.

First, the test set has been analysed with the aforementioned algorithm in order to verify the robustness of the method (fault-free case). No false alarm was observed. Second, the original test set was modified for performance evaluation. Indeed, the vibrations (frequency f) have been artificially added on the signal y only in the flight phases where the LCO is more likely to trigger on the elevator

³ The turbulence levels $T_1 - T_2 - T_3$ are three increasing levels of turbulence (low, medium and strong) assessed with regard to Airbus pilots sensitivity.

(e.g., when the hinge moment of the control surface is close to 0, see also Fig. 3). In particular, we have considered three target levels A_1, A_2 and A_3 to be detected in this campaign (three target levels corresponding to three cockpit vibration levels: lower than pilot sensitivity A_1 , detectable by the average pilot $A_2 \approx 1.35A_1$, possible in-flight turn back $A_3 \approx 2.2A_1$, see Fig. 4). An example of one of the simulated scenarios for performance evaluation is shown in Fig. 5 with the control surface hinge moment. Almost 170 different flight conditions were considered for this scenario according to Table 1. An auto-recursive Simulink model was chosen to implement the algorithm and to evaluate its performance in terms of detection and estimation capabilities (we want to estimate amplitude and duration for the diagnostic objective as explained in Section 4). Fig. 6 shows an example of application of the algorithm for the target amplitude A_2 . We can observe that the vibration is always detected⁴. However, the estimation accuracy in terms of amplitude and duration depends on the particular flight condition (the same is true for the other target amplitudes). In Fig. 8 we can observe a bar plot of the mean estimation errors⁵ as a function of the target amplitudes A_1, A_2, A_3 and for a low level of turbulence T_1 . It can be seen that the estimation errors are not monotone functions of the amplitude. In Fig. 9 we can observe a bar plot of the mean estimation errors as a function of the turbulence level ($T_1 = \text{low}, T_2 = \text{medium}, T_3 = \text{strong}$) for the target amplitude A_2 . As expected, the turbulence acts as an undesired interference for the detector and the estimation performance decreases as the turbulence level increases. It is interesting to observe that, from the analysis of Fig. 8 and 9, one can derive also a rough estimate of the propagation error on the predictive index in Section 4. Indeed, if we consider that $I(F)/k_w \approx \widehat{\Delta T} \hat{A}^2$, assuming no correlation⁶, the propagation error can be estimated as

$$e(I)/k_w \approx \sqrt{e(\widehat{\Delta T})^2 + (2e(\hat{A}))^2}.$$

Looking for example at Fig. 8, for the target level A_1 and A_2 , one would obtain $e(I)/k_w \approx 27\%$ and $e(I)/k_w \approx 6\%$.

6. CONCLUSION

This paper studies a statistical approach for the detection and diagnosis of a particular type of vibration, called Limit Cycle Oscillation (LCO), impacting the control surface of a civil aircraft. The idea is to detect the LCO using a generalized likelihood ratio test and then to estimate the amplitude and duration of the oscillation to derive a predictive maintenance index. Indeed, knowing the status and trend of the LCO energy, one can estimate the degradation of the system due to LCO (wear process) and finally propose to the airlines a maintenance action on the short or long term. A straightforward method compliant with real-time implementation constraint was proposed and a Monte Carlo test campaign was performed in order to assess the robustness and the detection/estimation

⁴ Please note that for industrial confidentiality reasons the real amplitudes are not shown, but the Signal to Noise Ratio (SNR) justifies the use of statistical test as the GLRT.

⁵ For a generic flight condition n , the normalized error is defined as: $Error(n) = (\text{True Value} - \text{Estimated Value})/\text{True Value}$.

⁶ only for the purpose of getting a simple estimate even if it is generally not true

performance of the algorithm. Further studies have to be carried out concerning the threshold tuning process for the predictive index and to extend the flight conditions encountered in the Monte Carlo test campaign.

REFERENCES

Dowell, H. (2014). *A Modern Course in Aeroelasticity: Fifth Revised and Enlarged Edition*. Solid Mechanics and Its Applications. Springer International Publishing.

Galy, J., Chaumette, E., and Larzabal, P. (2010). Joint detection estimation problem of monopulse angle measurement. *IEEE Transactions on Aerospace and Electronic Systems*, 46(1), 397–413.

Goupil, P. (2010). Oscillatory failure case detection in the A380 electrical flight control system by analytical redundancy. *Control Engineering Practice*, 18(9), 1110–1119.

Goupil, P., Urbano, S., and Tourneret, J.Y. (2016). A data-driven approach to detect faults in the airbus flight control system. *Proceedings of the 20th IFAC Symposium on Automatic Control in Aerospace, IFAC-PapersOnLine*, 49(17), 52–57.

Kay, S.M. (1993). *Fundamentals of statistical signal processing, volume 1: Estimation theory*. Prentice Hall.

Kay, S.M. (1998). *Fundamentals of statistical signal processing, volume 2: Detection theory*. Prentice Hall.

Livne, E. (2017). Aircraft active flutter suppression state of the art and technology maturation needs. *58th AIAA/ASCE/AHS/ASC Structures, Structural Dynamics, and Materials Conference, AIAA SciTech Forum*.

Safi, S., Kelly, D., and Archer, R. (2002). Interaction between wear processes and limit cycle oscillations of a control surface with free-play non-linearity. *Proceedings of the Institution of Mechanical Engineers, Part G: Journal of Aerospace Engineering*, 216(3), 143–153.

Scharf, L.L. and Friedlander, B. (1994). Matched subspace detectors. *IEEE Transactions on signal processing*, 42(8), 2146–2157.

Simon, P. (2011). *Détection robuste et précoce des pannes oscillatoires dans les systèmes de commandes de vol*. Ph.D. thesis, Bordeaux 1.

Stoica, P. and Nehorai, A. (1990). Performance study of conditional and unconditional direction-of-arrival estimation. *IEEE Transactions on Acoustics, Speech, and Signal Processing*, 38(10), 1783–1795.

Urbano, S., Chaumette, E., Goupil, P., and Tourneret, J.Y. (2017a). A data-driven approach for actuator servo loop failure detection. *Proceedings of the 20th IFAC World Congress, IFAC-PapersOnLine*, 50(1), 13544–13549.

Urbano, S., Chaumette, E., Goupil, P., and Tourneret, J.Y. (2017b). Performance of the generalized likelihood ratio test for the conditional observation model in the asymptotic region. *Submitted to IEEE Transactions on Signal Processing*.

Van Trees, H.L. (2004). *Detection, estimation, and modulation theory*. John Wiley & Sons.

Von Baumhauer, A. and Koning, C. (1923). On the stability of oscillations of an airplane wing. *National Advisory Committee for Aeronautics (NACA), Technical Memorandum n.223*.

Ziskind, I. and Wax, M. (1988). Maximum likelihood localization of multiple sources by alternating projection. *IEEE Transactions on Acoustics, Speech, and Signal Processing*, 36(10), 1553–1560.

Zolghadri, A., Henry, D., Cieslak, J., Efimov, D., and Goupil, P. (2013). *Fault diagnosis and fault-tolerant control and guidance for aerospace vehicles: from theory to application*. Springer Science & Business Media.

Table 1. Considered Operating Conditions.

Parameters	Range
Mass	63-95% Maximum takeoff weight
Balance	20-40%
Mach	0.6-0.8
Turbulence	$T_1 - T_2 - T_3$

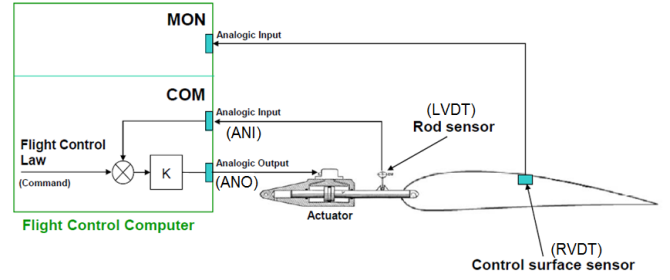


Fig. 1. Airbus control surface servo loop.

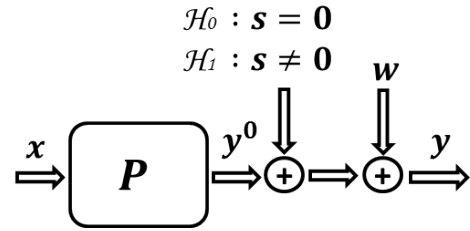


Fig. 2. Control surface servo loop model.

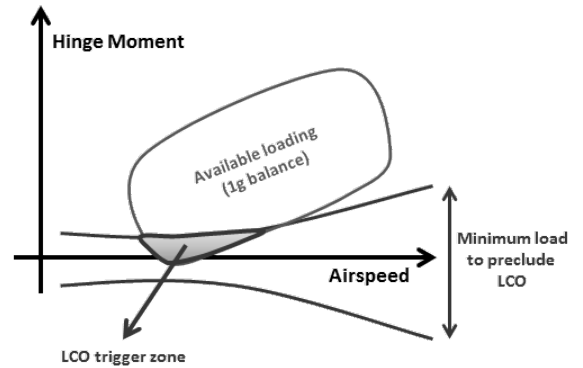


Fig. 3. LCO trigger zone based on control surface hinge moment.

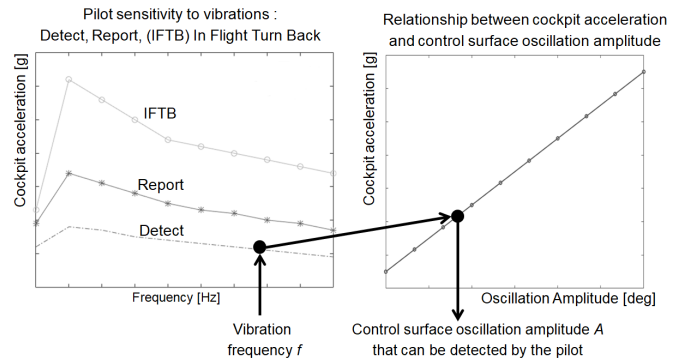


Fig. 4. Example of identification for the vibration target level A_2 .

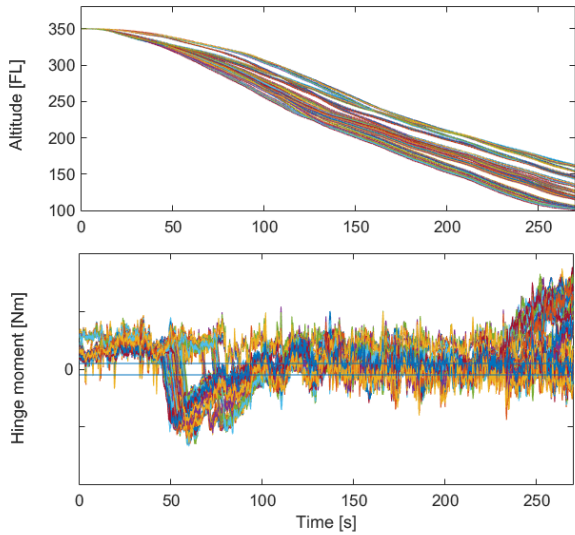


Fig. 5. Aircraft descent under different operating conditions: altitude (up) and control surface hinge moment (down). The hinge moment values are hidden for confidentiality reasons.

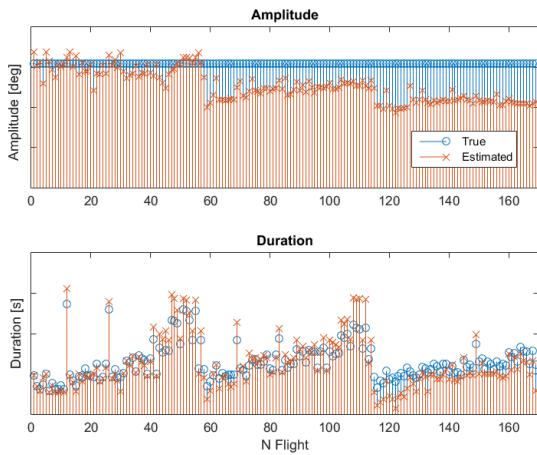


Fig. 6. Example of amplitude estimation (up) and duration estimation (down) for the simulated scenario in Fig. 5 and the target amplitude A_2 .

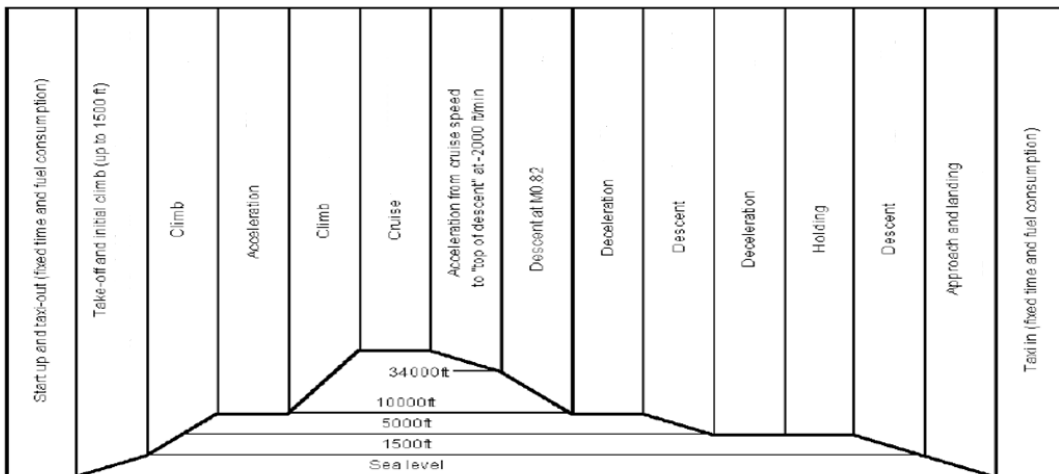


Fig. 7. Typical vertical flight path.

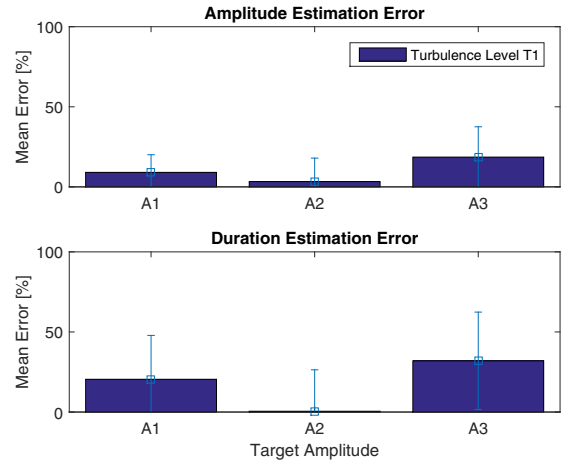


Fig. 8. Mean amplitude estimation error (up) and mean duration estimation error (down) for the case in Figure 5 as a function of the target amplitude for a low level of turbulence. A 2σ error bar is also considered for each mean error.

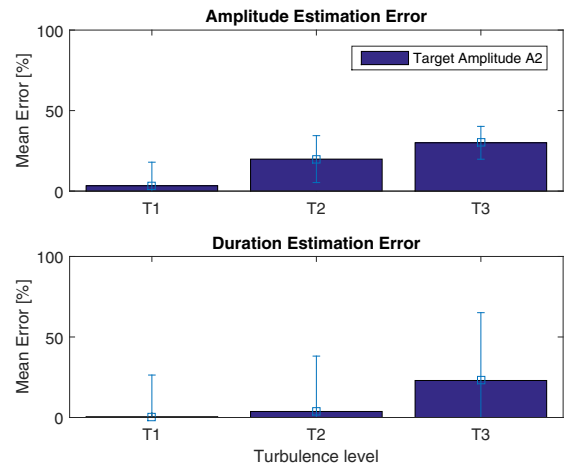


Fig. 9. Mean amplitude estimation error (up) and mean duration estimation error (down) for the case in Fig. 5 as a function of the turbulence level for the target amplitude A_2 . A 2σ error bar is also considered for each mean error.

Appendix A. TEST PERFORMANCE

The expression of the parameters r and k in (9), depends on the knowledge of the vector $\boldsymbol{\alpha}$. Indeed, it can be proved (Kay, 1998) that for a known vector $\boldsymbol{\alpha}$ we obtain

$$r = \text{rank}(\mathbf{H}_s)$$

$$k = \frac{\boldsymbol{\beta}_1^T \mathbf{H}_1^T(\boldsymbol{\alpha}_1) \Pi_{\mathbf{H}_0(\boldsymbol{\alpha}_0)}^\perp \mathbf{H}_1(\boldsymbol{\alpha}_1) \boldsymbol{\beta}_1}{\sigma^2}$$

For an unknown vector $\boldsymbol{\alpha}$, the equations (9) are verified only in the asymptotic region, i.e., at high Signal to Noise Ratio (SNR), we have (Urbano et al., 2017b)

$$k = \frac{\boldsymbol{\beta}_1^T \mathbf{H}_1^T(\boldsymbol{\alpha}_1) \mathbf{L}_0^\perp \mathbf{H}_1(\boldsymbol{\alpha}_1) \boldsymbol{\beta}_1}{\sigma^2}$$

$$r = \text{rank}(\mathbf{L}_0^\perp - \mathbf{L}_1^\perp)$$

where

$$\mathbf{L}_0^\perp = \Pi_{\mathbf{H}_0(\boldsymbol{\alpha}_0)}^\perp \Pi_{\mathbf{D}_0}^\perp \Pi_{\mathbf{H}_0(\boldsymbol{\alpha}_0)}^\perp, \quad \mathbf{D}_0 = \Pi_{\mathbf{H}_0(\boldsymbol{\alpha}_0)}^\perp \frac{\partial \mathbf{H}_0(\boldsymbol{\alpha}_0) \boldsymbol{\beta}_0}{\partial \boldsymbol{\alpha}_0}$$

$$\mathbf{L}_1^\perp = \Pi_{\mathbf{H}_1(\boldsymbol{\alpha}_1)}^\perp \Pi_{\mathbf{D}_1}^\perp \Pi_{\mathbf{H}_1(\boldsymbol{\alpha}_1)}^\perp, \quad \mathbf{D}_1 = \Pi_{\mathbf{H}_1(\boldsymbol{\alpha}_1)}^\perp \frac{\partial \mathbf{H}_1(\boldsymbol{\alpha}_1) \boldsymbol{\beta}_1}{\partial \boldsymbol{\alpha}_1}$$

Appendix B. MLE AND TEST STATISTIC

The maximum likelihood estimates and the test statistic for (1) can be computed based on (5),(4) and (8) as

$$\hat{\boldsymbol{\alpha}}_0 = \hat{p}_0 = \underset{p}{\text{argmax}} (\mathbf{y}^T \mathbf{H}_0(\boldsymbol{\alpha}_0) (\mathbf{H}_0^T(\boldsymbol{\alpha}_0) \mathbf{H}_0(\boldsymbol{\alpha}_0))^{-1} \mathbf{H}_0^T(\boldsymbol{\alpha}_0) \mathbf{y})$$

$$= \underset{p}{\text{argmax}} \left(\frac{(\mathbf{x}^T(p) \mathbf{y})^2}{\mathbf{x}^T(p) \mathbf{x}(p)} \right)$$

$$\hat{\boldsymbol{\beta}}_0 = \hat{\lambda}_0 = (\mathbf{H}_0^T(\hat{\boldsymbol{\alpha}}_0) \mathbf{H}_0(\hat{\boldsymbol{\alpha}}_0))^{-1} \mathbf{H}_0^T(\hat{\boldsymbol{\alpha}}_0) \mathbf{y} = \frac{\mathbf{x}^T(\hat{p}_0) \mathbf{y}}{\mathbf{x}^T(\hat{p}_0) \mathbf{x}(\hat{p}_0)}$$

$$\hat{\boldsymbol{\alpha}}_1 = \left(\begin{array}{c} \hat{p}_1 \\ \hat{f} \end{array} \right) = \underset{p, f}{\text{argmax}} (\mathbf{y}^T \mathbf{H}_1(\boldsymbol{\alpha}_1) (\mathbf{H}_1^T(\boldsymbol{\alpha}_1) \mathbf{H}_1(\boldsymbol{\alpha}_1))^{-1} \mathbf{H}_1^T(\boldsymbol{\alpha}_1) \mathbf{y})$$

$$\underset{N \rightarrow \infty}{=} \underset{p, f}{\text{argmax}} \left(\frac{(\mathbf{x}^T(p) \mathbf{y})^2 + 2(\mathbf{x}^T(p) \mathbf{x}(p)) I_y(f)}{-4(\mathbf{x}^T(p) \mathbf{y}) \text{Re}[I_{xy}(f)] - 4(\text{Im}[I_{xy}(f)])^2} \right)$$

$$\hat{\boldsymbol{\beta}}_1 = \left(\begin{array}{c} \hat{\lambda}_1 \\ \hat{l}_1 \\ \hat{l}_2 \end{array} \right) = (\mathbf{H}_1^T(\hat{\boldsymbol{\alpha}}_1) \mathbf{H}_1(\hat{\boldsymbol{\alpha}}_1))^{-1} \mathbf{H}_1^T(\hat{\boldsymbol{\alpha}}_1) \mathbf{y}$$

$$= \left(\begin{array}{c} \frac{\mathbf{x}^T(\hat{p}_1) \mathbf{y} - 2 \text{Re}[I_{xy}(\hat{f})]}{\mathbf{x}^T(\hat{p}_1) \mathbf{x}(\hat{p}_1) - 2 I_x(\hat{f})} \\ \left(\frac{\frac{2}{N} (\mathbf{x}^T(\hat{p}_1) \mathbf{x}(\hat{p}_1)) \mathbf{c}^T(\hat{f}) (\mathbf{y} - r'(\hat{p}_1) \mathbf{x}(\hat{p}_1)) + \frac{4}{N} (\mathbf{x}^T(\hat{p}_1) \mathbf{s}(\hat{f})) \text{Im}[I_{xy}(\hat{f})]}{\mathbf{x}^T(\hat{p}_1) \mathbf{x}(\hat{p}_1) - 2 I_x(\hat{f})} \right) \\ \left(\frac{\frac{2}{N} (\mathbf{x}^T(\hat{p}_1) \mathbf{x}(\hat{p}_1)) \mathbf{s}^T(\hat{f}) (\mathbf{y} - r'(\hat{p}_1) \mathbf{x}(\hat{p}_1)) - \frac{4}{N} (\mathbf{x}^T(\hat{p}_1) \mathbf{c}(\hat{f})) \text{Im}[I_{xy}(\hat{f})]}{\mathbf{x}^T(\hat{p}_1) \mathbf{x}(\hat{p}_1) - 2 I_x(\hat{f})} \right) \end{array} \right)$$

$$T'' = \left(\left\| \Pi_{\mathbf{H}_1(\hat{\boldsymbol{\alpha}}_1)} \mathbf{y} \right\|^2 - \left\| \Pi_{\mathbf{H}_0(\hat{\boldsymbol{\alpha}}_0)} \mathbf{y} \right\|^2 \right)$$

$$= \left(\frac{(\mathbf{x}^T(\hat{p}_1) \mathbf{y})^2 + 2(\mathbf{x}^T(\hat{p}_1) \mathbf{x}(\hat{p}_1)) I_y(\hat{f}) - 4(\mathbf{x}^T(\hat{p}_1) \mathbf{y}) \text{Re}[I_{xy}(\hat{f})] - 4(\text{Im}[I_{xy}(\hat{f})])^2}{(\mathbf{x}^T(\hat{p}_1) \mathbf{x}(\hat{p}_1) - 2 I_x(\hat{f}))} - \frac{(\mathbf{x}^T(\hat{p}_0) \mathbf{y})^2}{\mathbf{x}^T(\hat{p}_0) \mathbf{x}(\hat{p}_0)} \right) \stackrel{\mathcal{H}_0}{\leq} 2\sigma^2 \gamma$$

where

$$r'(p) = \frac{\mathbf{x}^T(p) \mathbf{y}}{\mathbf{x}^T(p) \mathbf{x}(p)}$$

and where the terms $I_x(f)$ and $I_y(f)$ are the periodograms of \mathbf{x} and \mathbf{y}

$$I_x(f) = \frac{1}{N} [(\mathbf{c}^T(f) \mathbf{x})^2 + (\mathbf{s}^T(f) \mathbf{x})^2]$$

$$I_y(f) = \frac{1}{N} [(\mathbf{c}^T(f) \mathbf{y})^2 + (\mathbf{s}^T(f) \mathbf{y})^2]$$

Note that $\text{Re}[I_{xy}(f)]$ and $\text{Im}[I_{xy}(f)]$ are the real and the imaginary parts of the cross-periodogram $I_{xy}(f)$ (also referred to as co-periodogram and quadrature periodogram)

$$I_{xy}(f) = \frac{1}{N} [(\mathbf{c}^T(f) \mathbf{x} - i \mathbf{s}^T(f) \mathbf{x})(\mathbf{c}^T(f) \mathbf{y} + i \mathbf{s}^T(f) \mathbf{y})]$$

$$\text{Re}[I_{xy}(f)] = \frac{1}{N} [(\mathbf{c}^T(f) \mathbf{x})(\mathbf{c}^T(f) \mathbf{y}) + (\mathbf{s}^T(f) \mathbf{x})(\mathbf{s}^T(f) \mathbf{y})]$$

$$\text{Im}[I_{xy}(f)] = \frac{1}{N} [(\mathbf{c}^T(f) \mathbf{x})(\mathbf{s}^T(f) \mathbf{y}) - (\mathbf{s}^T(f) \mathbf{x})(\mathbf{c}^T(f) \mathbf{y})]$$

Note also that a large sample approximation has been considered for the derivation of $\hat{\boldsymbol{\beta}}_1$ and $\hat{\boldsymbol{\alpha}}_1$. In this case, when f is not too close to 0 or $1/2$ (otherwise the parameters are not identifiable), the following approximations can be made $\mathbf{c}^T \mathbf{c}/N \approx 1/2$, $\mathbf{s}^T \mathbf{s}/N \approx 1/2$ and $\mathbf{c}^T \mathbf{s}/N \approx 0$.

Note: If we cannot guarantee the absence of signal power at the frequency \hat{f} in \mathbf{x} , but we can consider that the power of the anomaly is small compared to the energy and covariance terms $\mathbf{x}^T(\hat{p}) \mathbf{x}(\hat{p})$ and $\mathbf{x}^T(\hat{p}) \mathbf{y}$, we can say that $\hat{p}_0 \approx \hat{p}_1 \approx \hat{p}$ and that $(\text{Im}[I_{xy}(\hat{f})])^2 \approx 0$ being a second order term in $\text{Re}[I_x(\hat{f})]$ and $\text{Im}[I_x(\hat{f})]$. The sufficient statistic of our detection problem will takes the following simplified form

$$T''' = (I_y(\hat{f}) - 2r'(\hat{p}) \text{Re}[I_{xy}(\hat{f})]) > \sigma^2 \gamma''$$

whose dominant term is still the periodogram of \mathbf{y} , but corrected by an additional term representing the correlation between \mathbf{x} and \mathbf{y} (in the time and frequency domain). In a further simplified version of the algorithm, the estimation of the system dynamic P and the detection of the anomaly \mathbf{s} can be decoupled, leading to a two step approach of the type: estimation of the system dynamic for residual generation ($\mathbf{y} - \widehat{\mathbf{y}}^0$) plus sinusoidal detection on the residuals (e.g., maximum of the periodogram on the residuals).